

UDP-glucose Dehydrogenase Plays Multiple Roles in the Biology of the Pathogenic Fungus *Cryptococcus neoformans**

Received for publication, August 4, 2004, and in revised form, September 9, 2004
Published, JBC Papers in Press, September 21, 2004, DOI 10.1074/jbc.M408889200

Cara L. Griffith[‡], J. Stacey Klutts^{‡§¶}, Lijuan Zhang^{§||}, Steven B. Levery^{**†‡},
and Tamara L. Doering^{‡§§}

From the Departments of [‡]Molecular Microbiology and [§]Pathology and Immunology, Washington University School of Medicine, St. Louis, Missouri 63110 and the ^{**}Department of Chemistry, University of New Hampshire, Durham, New Hampshire 03824

Cryptococcus neoformans is a pathogenic fungus surrounded by an elaborate polysaccharide capsule that is strictly required for its virulence in humans and other mammals. Nearly half of the sugar residues in the capsule are derived from UDP-glucuronic acid or its metabolites. To examine the role of these nucleotide sugars in *C. neoformans*, the gene encoding UDP-glucose dehydrogenase was disrupted. Mass spectrometry analysis of nucleotide sugar pools showed that the resulting mutant lacked both UDP-glucuronic acid and its downstream product, UDP-xylose, thus confirming the effect of the knockout and indicating that an alternate pathway for UDP-glucuronic acid production was not used. The mutant was dramatically affected by the lack of specific sugar donors, demonstrating altered cell integrity, temperature sensitivity, lack of growth in an animal model of cryptococcosis, and morphological defects. Additionally, the polysaccharide capsule could not be detected on the mutant cells, although the possibility remains that abbreviated forms of capsule components are made, possibly without proper surface display. The capsule defect is largely independent of the other observed changes, as cells that are acapsular because of mutations in other genes show lack of virulence but do not exhibit alterations in cell integrity, temperature sensitivity, or cellular morphology. All of the observed alterations were reversed by correction of the gene disruption.

To fully understand the biosynthesis of polysaccharides, it is necessary to investigate the upstream sources of their component sugars. In many cases the immediate donors are nucleotide sugars, the activated forms of monosaccharides that are the substrates of glycosyl transfer reactions. These compounds may be formed from appropriate monosaccharides or sugar phosphates or generated through interconversion of existing nucleotide sugars. An example of the latter case is the pathway

centered on UDP-glucuronic acid (UDP-GlcUA).¹ This compound is generated from UDP-glucose via the action of UDP-glucose dehydrogenase (Ugd1p) and depending on the cell type may be further converted to UDP-xylose, UDP-arabinose, UDP-galacturonic acid, or other compounds (reviewed in Ref. 1).

The broad importance of UDP-GlcUA is readily apparent upon consideration of the downstream polymers that utilize this compound or its immediate descendents. For example, bacterial cells require the formation of UDP-aminoarabinose from UDP-GlcUA for lipid A modifications that occur in the setting of resistance to antimicrobial peptides (2). Matrix polysaccharides in plants, which are constitutively synthesized to maintain cell wall integrity, may derive half of their mass from monosaccharides donated from UDP-GlcUA derivatives (3). In animals, synthesis of glycoproteins and proteoglycans is dependent on UDP-xylose and other compounds generated from UDP-GlcUA.

Our interest in UDP-glucuronic acid arises from its importance in capsule synthesis in the pathogenic fungus *Cryptococcus neoformans*. This opportunistic pathogen causes severe disease in immunocompromised individuals, which is generally fatal if not treated. For virulence, this organism depends on an extensive polysaccharide capsule that surrounds its cell wall. One capsule component is termed galactoxylomannan (GalXM), a polymer in which about 20 mol % of the sugar residues are xylose (4). The majority of the capsule is composed of a second polymer termed glucuronoxylomannan (GXM), which consists of an α -1,3-linked mannose backbone modified with monomeric side chains of xylose and glucuronic acid. The xylose and glucuronic acid of GXM account for 40–60% of the total sugars in this polymer, depending on the serotype (5). The heavy modification with glucuronic acid contributes to the highly acidic nature of GXM, and thus of the fungal cell surface. The xylose residues of GXM have been shown to be required for normal virulence of the cells (6).

Motivated by the requirement for capsule in cryptococcal pathogenesis, and by the importance of UDP-glucuronic acid in capsule synthesis, we wished to investigate the effects on cryptococcal biology and virulence of reducing the levels of this nucleotide sugar. To do this we deleted the fungal gene encoding UDP-glucose dehydrogenase. This protein has been the subject of intensive study, including its purification and cloning

* This work was supported in part by National Institutes of Health Grant GM R01 066303 and a Burroughs Wellcome Fund Junior Investigator in Molecular Pathogenic Mycology award (to T. L. D.). The costs of publication of this article were defrayed in part by the payment of page charges. This article must therefore be hereby marked "advertisement" in accordance with 18 U.S.C. Section 1734 solely to indicate this fact.

¶ Supported by National Institutes of Health Grant GM F32 072341.

|| Supported by National Institutes of Health Grant GM R01 069968.

‡‡ Supported by National Institutes of Health Grant NCR R21 RR16459.

§§ To whom correspondence should be addressed: Campus Box 8230, 660 South Euclid Ave., St. Louis, MO 63110-1093. Tel.: 314-747-5597; Fax: 314-362-1232; E-mail: doering@wustl.edu.

¹ The abbreviations used are: GlcUA, glucuronic acid; Ugd1p, UDP-glucose dehydrogenase; DIC, differential interference contrast; GalXM, galactoxylomannan; GXM, glucuronoxylomannan; Uxs1p, UDP-glucuronic acid decarboxylase; MES, 4-morpholineethanesulfonic acid; HPLC, high pressure liquid chromatography; MS, mass spectrometry; GC, gas chromatography; MOPS, 4-morpholinepropanesulfonic acid; wt, wild type.

from multiple prokaryotic and eukaryotic organisms (reviewed in Ref. 7) and analysis of its three-dimensional structure (7). We previously examined the characteristics of the cryptococcal enzyme, establishing kinetic parameters for the wild type and several mutant forms (8). We also noted that the cryptococcal protein occurs as a dimer, similar to the case in bacteria (9) but unlike other eukaryotes that have been investigated (10–13). In this study we examine the effects of deleting the gene encoding Ugd1p on nucleotide sugar pools, capsule synthesis, cell growth, and fungal virulence.

EXPERIMENTAL PROCEDURES

Strains and Cell Growth—The *cas2* mutant strain NE146 and the *uxs1* mutant strain NE178 were provided by Guilhem Janbon (Institute Pasteur); the *cap59* mutant strain TYCC33 was from June Kwon-Chung (National Institutes of Health), and the wild type *C. neoformans* strain JEC21 (serotype D MAT α) was provided by Joe Heitman (Duke University). Cells in liquid culture were grown at 30 °C with continuous shaking in YP medium (1% BactoYeast Extract, 2% BactoPeptone) containing 2% dextrose or 2% *myo*-inositol as noted. For phenotypic analysis, cells were grown overnight, diluted to an A_{600} of 1, and allowed to grow for another hour. Cells were then further diluted to an A_{600} of 0.1, and 5- μ l aliquots of this suspension and three 5-fold serial dilutions in deionized H₂O were plated. Growth conditions tested included YPD, minimal medium, and YPD supplemented with 1 M sorbitol, 0.005% SDS, 1 M NaCl, 50 mM MES, pH 5.5, 50 mM Tris, pH 8.8, or 30 μ g/ml Congo Red (Sigma). Growth was assessed at 25, 30, or 37 °C as noted in the text.

UGD1 Disruption and Complementation—Gene disruption was carried out essentially as described previously (14). The disruption construct contained the entire UDP-glucose dehydrogenase gene (*UGD1*; GenBank™ accession number AF405548) with bp 840–1080 (including the region encoding a conserved cysteine that is required for activity (8)) replaced by the nourseothricin acetyltransferase coding sequence from *Streptomyces noursei* (*nat1*) to confer nourseothricin resistance (15). To make this construct, *UGD1* was PCR-amplified from serotype D strain JEC43 α genomic DNA using sense primer DH-21 (5'-TCGCTCGTTCT-TCGGTGCAGCTG-3') and antisense primer DH-1 (5'-CAGAAAAC-TAGCAGCAATGTTGGG-3'). The 2649-bp product was gel-purified and cloned into pCR2.1-TOPO (Invitrogen). The C-terminal 1424 bp of *UGD1* were removed by digestion with EcoRV and cloned into plasmid GMC-200-MCS to form plasmid Nat/DH. (GMC-200-MCS is a modification of GMC-200 (provided by Gary Cox, Duke University Medical Center), which contains *nat1* driven by a cryptococcal actin promoter that is preceded by a PmeI site. The *nat1* is followed by a Trp terminator which ends in an EcoRV restriction site, and the PmeI and EcoRV sites are flanked by PvuII sites.) The N-terminal 898-bp fragment of *UGD1* was PCR-amplified from genomic DNA and modified with terminal PmeI restriction sites using sense primer DH-PmeI (5'-GGGTTTAAAC-CCCACCAAACGCTTACATCC-3') and antisense primer DH-PmeI (5'-GGGTTTAAACCCCAAGTGGCAGCGTAGCC-3'). The product was column purified (Qiagen; Valencia, CA) and cloned into the GMC Nat/DH plasmid at PmeI. The final construct (DH/Nat/DH) contained the *UGD1* gene fragments in the same orientation as the *nat1* gene. This was digested with PvuII to release the DH/Nat/DH fragment, which was gel-purified and used to biologically transform JEC21 cells as in Refs. 16 and 17. The cells were allowed to recover on YPD medium for 24 h, replated onto YPD plates containing 100 μ g/ml nourseothricin, and incubated at 30 °C for 7–10 days to allow colony growth. To assess gene replacement, genomic DNA prepared from individual transformants was screened by PCR, using standard conditions with the addition of 5% Me₂SO (15). The oligonucleotides used, diagrammed in Fig. 1, panel A, are as follows: primer 1, 5'-CATGTCTCGTTTCTTCGTTCC-3'; primer 2, 5'-CCTTCTTGAAGGCCCAACCAAGAATCG-3'; primer 3, 5'-CCTATCCGATAAGGAACCG-3'; primer 4, 5'-CAGTCTGCAGG-GCACGGTGG-3'; and primer 5, 5'-CCGCCGGTACGCGTGGATCGCC-GG-3'. Several transformants were additionally tested by DNA blotting (below) to confirm gene replacement.

To complement the disruption strain we used a DNA fragment containing a hygromycin resistance gene (*HYG* (18)) and the entire coding sequence of *UGD1* along with 600 bp upstream as a putative promoter region. To make this fragment, *UGD1* plus the upstream region was PCR-amplified from JEC21 genomic DNA such that NotI and AvrII sites were added to the 5' end and a NotI site was added to the 3' end, using sense primer DH CB-1 (5'-ATAAGAATGCGGCCGCCCTAGGAA-CATTGCTCGTTGTTACTC-3') and antisense primer DH CB-2 (5'-

ATAAGAATGCGGCCGCCGACTATCGCCTTAAATACG-3'). The product was gel-purified and cloned into the pTEL-HYG plasmid (from Gary Cox (18)) at the NotI site. The resulting plasmid was digested with BamHI and AvrII to release a fragment containing both genes. This fragment was gel-purified and biologically delivered into the *ugd1* disruption strain. The cells were allowed to recover on YPD medium for 24 h, replated onto YPD plates containing 30 μ g/ml hygromycin B (Roche Diagnostics), and incubated at 30 °C for 7–10 days to allow colony growth. Colonies were screened by PCR and blotting as above.

DNA Blotting—Genomic DNA was isolated from wild type (JEC21), disruption strains, and corrected strains, digested overnight with XbaI, and probed with a 600-bp portion of *UGD1* (downstream of the *nat1* insertion site, hatched bar in Fig. 1, panel A) using standard methods (19). The probe was generated by PCR amplification using primers DH-2 (5'-TCCTTGGCCGAGGGTACCGCTATC-3') and DH-3 (5'-CCT-TCTTGAAGGCCCAACCAAGAATCG-3'), column-purified, and labeled with [α -³²P]dATP using the Random Primers DNA Labeling System (Invitrogen).

Isolation of Nucleotide Sugars—Nucleotide sugar pools from the various cryptococcal strains were isolated by ion-pair solid-phase extraction (20) of soluble fractions generated as described below under "Localization and Immunoblotting." Aliquots of these fractions corresponding to 1 mg of protein were brought to 1 ml with 10 mM ammonium bicarbonate and applied to 3-ml Envi-Carb carbon columns (Supelco; Bellefonte, PA) that had been pre-washed with 3 ml of 80% (v/v) acetonitrile in 0.1% (v/v) trifluoroacetic acid followed by 2 ml of water. To remove salts, detergents, and other unwanted solutes, the columns were sequentially washed with 2 ml of water, 2 ml of 25% (v/v) acetonitrile, and 2 ml of 50 mM TEAA buffer, pH 7 (Sigma). The nucleotide sugars were then eluted with 3 ml of 25% (v/v) acetonitrile in 50 mM TEAA buffer, pH 7. To remove the acetonitrile, samples were dried for 30 min under a stream of nitrogen, after which the aqueous remainder was lyophilized. The dried material was then sequentially redissolved in 1 ml of methanol, 0.5 ml of water, and 0.5 ml of methanol, with drying under nitrogen in between. The final dry samples were dissolved in 20 μ l of water, and 0.2 μ l of each was subjected to capillary HPLC-coupled mass spectrometry analysis.

Capillary HPLC—Capillary HPLC coupled to mass analysis was performed as described previously (21) with slight modifications, using an Agilent 1100 series capillary HPLC work station (Agilent) with Chemstation software for data acquisition, analysis, and management. HPLC separations were performed on a 0.3 \times 250-mm C18 column (Zorbax 300 SB, 5 μ m, Agilent) using a binary solvent system composed of 5% methanol (eluent A) and 90% methanol in water (eluent B), both containing 3.5 mM dibutylamine, with pH adjusted to 5.5 with 2 M acetic acid. After injection of 0.2 μ l of sample, the elution profile was 0% eluent B for 7 min, 15% eluent B for 9 min, 40% eluent B for 11 min, and 100% eluent B for 23 min. The flow rate was 5 μ l/min, and absorbances at 232, 260, and 280 nm were monitored during each run. After each run the column was washed with 90% eluent B for 15 min, and equilibrated with 100% eluent A for 40 min. The capillary HPLC was directly coupled to the mass spectrometer described below.

Mass Spectrometry—Mass spectra were acquired on a Mariner Bio-Spectrometry work station electrospray ionization time-of-flight mass spectrometer (PerSeptive Biosystems, Framingham, MA) in the negative ion mode as described previously (21, 22). Nitrogen was used as a desolvation gas as well as a nebulizer. Conditions for electrospray ionization-MS were as follows: nebulizer flow 1 liter/min, nozzle temperature 140 °C, drying gas (N₂) flow 0.1 liters/min, spray tip potential 2.8 kV, nozzle potential 70 V, and skimmer potential 9 V. Negative ion spectra were generated by scanning the range of m/z 150–1000. During analyses, the indicated vacuum was 2.1×10^{-6} torr. Total ion chromatograms and mass spectra were processed with the Data Explorer software version 3.0.

Immunofluorescence—To image capsule, cells were labeled for 60 min at room temperature as described previously (23) with either anticapsular monoclonal antibody 2H1 (from Arturo Casadevall), which was tagged with Cy3, or with unlabeled monoclonal antibodies to GXM (from Tom Kozel, listed in Table II), followed by washing and a second incubation with Cy3 tagged anti-mouse IgG (Molecular Probes, Eugene, OR). Images were obtained using a LSM510 laser scanning confocal microscope (Zeiss, Germany).

Transmission Electron Microscopy—For ultrastructural analysis, yeast cells were fixed for 1 h at room temperature in 2% glutaraldehyde (Polysciences Inc., Warrington, PA) in 100 mM phosphate buffer, pH 7.2. Cells were washed in phosphate buffer and postfixed for 1 h in 1% osmium tetroxide (Polysciences Inc.) and then rinsed in phosphate buffer and dehydrated in a graded series of ethanol and propylene oxide

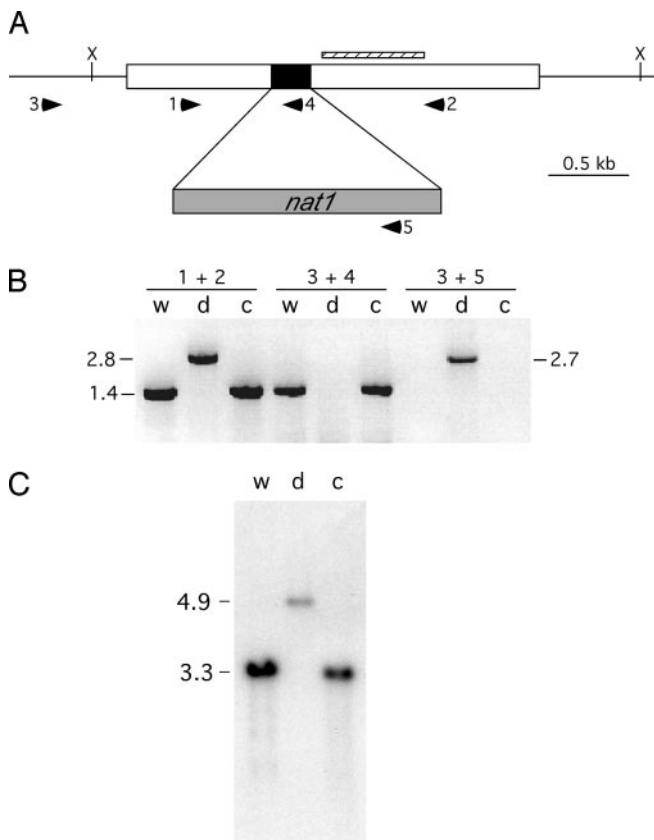


FIG. 1. Disruption of *UGD1* by biolistic transformation. *Panel A*, diagram of the disruption strategy, in which 0.24 kb (black box) of the *UGD1* coding sequence (white) was replaced with the 1.7-kb *nat1* cassette (gray, includes promoter and terminator as described under "Experimental Procedures"). *Panel B*, PCR of genomic DNA from wild type parental (*w*), disruption (*d*), and corrected (*c*) strains using the primers indicated above each triplet of lanes. Primer positions are indicated in *panel A*. *Panel C*, genomic DNA blot of wild type parental (*w*), disruption (*d*), and corrected (*c*) strains probed with a segment of *UGD1* that is retained in the disruption (narrow hatched bar in *panel A*).

prior to embedding in Eponate 12 resin (Ted Pella Inc., Redding, CA). Sections of 70–90 nm were cut with a Leica Ultracut UCT ultramicrotome (Leica Microsystems Inc., Bannockburn, IL), stained with uranyl acetate and lead citrate, and viewed with a JEOL 1200EX transmission electron microscope (JEOL Inc., Peabody, MA).

Compositional Analysis—Glycosyl residue composition was determined by gas chromatography/mass spectrometry (GC/MS) of the per-*O*-trimethylsilyl methyl glycosides obtained by methanolysis of polysaccharide samples, essentially as described by Merkle and Poppe (24). Briefly, methanolysis was performed by treatment of dried aliquots of polysaccharide with 1 N HCl in anhydrous methanol (1.0 ml, 80 °C, 16–22 h). Per-*O*-trimethylsilylation of the resultant monosaccharide methyl glycosides was carried out using Tri-Sil (Pierce; 200 ml, 80 °C, 30 min). Following careful evaporation of the Tri-Sil, the trimethylsilyl methyl glycosides were extracted into *n*-hexane for GC/MS analysis using a 30-m DB-5-bonded phase fused silica capillary column or equivalent (splitless injection; temperature program 140–260 °C at 4 °C/min). GC/MS analysis was performed using a Finnigan GCQ GC/IT-MS operating in electron ionization mode. Glycoside derivatives were identified by characteristic retention times and mass spectra compared, where necessary, to those of authentic standards; quantitation was based on total ion current traces.

GXM Preparation—Isolation of GXM was essentially as described by Cherniak *et al.* (25). Briefly, cells were grown at 30 °C with constant shaking for 5 days in capsule induction medium (35 mM MOPS, pH 7.1; 12 mM NaHCO₃; 2% (w/v) dextrose; 1.5 g/liter asparagine; 1.7 g/liter Yeast Nitrogen Base without amino acids and ammonium sulfate (Difco)). Cells were sedimented at 15,000 × *g* for 15 min at 4 °C, and any remaining cells were cleared from the supernatant fraction by filtration over a 0.22- μ m membrane. The polysaccharide was precipitated overnight with 3 volumes of 95% ethanol, subjected to centrifugation as before, and washed sequentially with 95% ethanol, acetone, and ether.

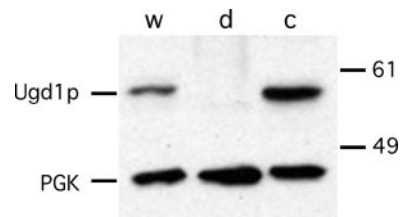


FIG. 2. Immunoblotting of Ugd1p. Total protein (10 μ g) from wild type (*w*), disruption (*d*), and corrected (*c*) strains was resolved by SDS-PAGE and transferred to nitrocellulose, which was then divided at the level of the 49-kDa marker. The upper part of the membrane was probed as described under the "Experimental Procedures" with polyclonal antibody to Ugd1p (8), and the lower part with antibody to PGK to serve as a loading control. Standards are indicated at right (in kDa). Regions of the blot that are not shown contained no additional specific bands when probed with either antibody.

The pellet was air-dried at room temperature, weighed, and then dissolved in 0.2 M NaCl (10 mg/ml) at 4 °C overnight with constant stirring. For every mg of polysaccharide, 3 mg of hexadecyltrimethylammonium bromide was added. Additional hexadecyltrimethylammonium bromide from a 0.05% solution was then slowly added until a precipitate appeared. The precipitate was spun at 10,000 × *g* for 15 min at room temperature, dried, weighed, and dissolved in 25 ml of 1 M NaCl as before. GXM was then precipitated with 95% ethanol as above, dissolved in 1 M NaCl, and finally dialyzed against tap water for 2 days and distilled water for 3 days. The sample was filtered over a 0.22- μ m membrane and lyophilized overnight. The typical yield from a 500-ml culture of wild type cells was 75 mg for wild type.

Localization and Immunoblotting—For membrane preparations, JEC21 cells were grown in 50 ml of YPD at 30 °C overnight and then harvested by centrifugation at 2,500 × *g* for 10 min at 4 °C and washed in 5 ml of cold lysis buffer (100 mM Tris-HCl, pH 8.0, and 0.1 mM EDTA). The cell pellet was resuspended in 2 ml of lysis buffer supplemented with 1 mM dithiothreitol and protease inhibitors (0.5 mM phenylmethylsulfonyl fluoride; 5 μ g/ml antipain, trypsin inhibitor, and leupeptin; 1 μ g/ml *o*-phenanthroline; 0.1 mM aminocaproic acid, and 1.6 μ g/ml benzamide). An equal volume of 0.5-mm glass beads (Biospec Products, Bartlesville, OK) was then added to the suspension, which was vigorously vortex mixed for 2 min alternating with 1 min on ice until >80% breakage was observed under a light microscope. The lysate was removed, and the beads were washed twice with 1 ml of lysis buffer. Washes were pooled with the remainder of the lysate, and the pool was subjected to a clearing spin (1,100 × *g*, 5 min, 4 °C). 0.5 ml of the supernatant was removed ("total protein fraction"), and the remainder was subjected to high speed centrifugation (60,000 × *g*, 45 min, 4 °C). The supernatant fraction was reserved ("soluble fraction"), and the membrane pellet was resuspended thoroughly in 1 ml of lysis buffer and spun again as before. The resulting crude washed membrane fraction was resuspended in lysis buffer. The soluble fraction was concentrated 8-fold using an Amicon Ultrafiltration device (Millipore, Billerica, MA), and all fractions were stored at 4 °C. Equal proportions of each fraction were boiled in SDS-PAGE sample buffer and resolved by SDS-PAGE on a 10% gel. Standard methods were used for transfer and immunoblotting, using dilutions of 1:5,000 for both primary antiserum (anti-Ugd1p (8) or anti-PGK (from Randy Shekman)) and secondary antiserum (anti-rabbit IgG conjugated to horseradish peroxidase; Amersham Biosciences), and detection with Western Lighting Chemiluminescence Reagent (PerkinElmer Life Sciences).

Animal Studies— 2.5×10^4 cells in 50 μ l of deionized H₂O were delivered intranasally into 4–6-week-old C57Bl/6 mice (NCI, National Institutes of Health). Groups of three and five mice were humanely sacrificed at 1 h and 7 days after inoculation, respectively. The lungs were harvested, homogenized in water, and plated for colony-forming units as described in Ref. 26.

RESULTS

To begin investigating the role of UDP-glucuronic acid in *C. neoformans* biology, we deleted the *UGD1* gene that encodes UDP-glucose dehydrogenase. To do this, we generated a construct in which a 240-bp segment of the gene (including the sequence encoding a conserved cysteine required for activity (8)) was replaced by a drug resistance marker (*nat1*), but 0.9 kb of 5' genomic sequence and 1.4 kb of 3' genomic sequence

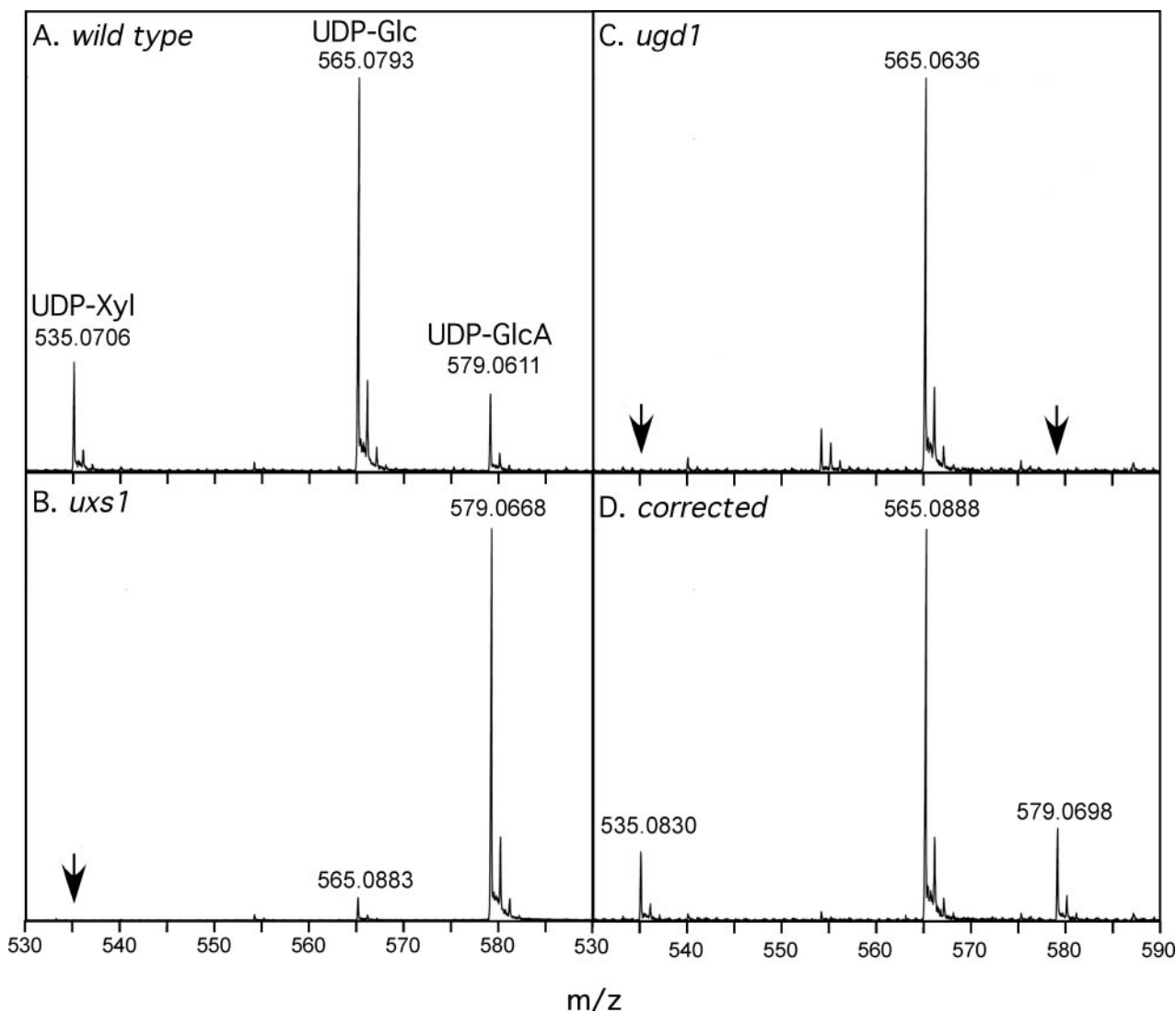


FIG. 3. **UDP-GlcUA and UDP-Xyl are not detectable in *ugd1* mutant cells.** Nucleotide sugars were extracted and analyzed as described under "Experimental Procedures," and portions of the mass spectra showing the z1 charge state peaks of these compounds are shown for wild type (panel A), *uxs1* mutant (panel B), *ugd1* mutant (panel C), and corrected *ugd1* cells (panel D). The UDP-Xyl peak is at 535.08, UDP-Glc at 565.07, and UDP-GlcUA at 579.07 mass units; and where no signal above background was detected at any one of these positions, that position is indicated with an arrow (panels B and C). Each panel is scaled to the highest peak, corresponding to the following total ion counts: panel A, UDP-Glc, 4102; panel B, UDP-GlcUA, 16,000; panel C, UDP-Glc, 2118; and panel D, UDP-Glc, 2128. Relative peak heights are provided in Table I.

TABLE I

UDP-GlcUA, UDP-Glc, and UDP-Xyl detected in wild type and mutant strains of *C. neoformans*

All ion counts are normalized to UDP-glucose (set arbitrarily to 100; actual counts provided in the legend for Fig. 3).

Cells tested	UDP-glucose	UDP-glucuronic acid	UDP-xylose
Wild type	100	27	20
<i>Uxs1</i>	100	1722	<0.9 ^a
<i>Ugd1</i>	100	<0.2 ^a	<0.2 ^a
<i>UGD1</i>	100	24	18

^a The observed ion counts for these compounds were equal to background levels for the spectra (see Fig. 3).

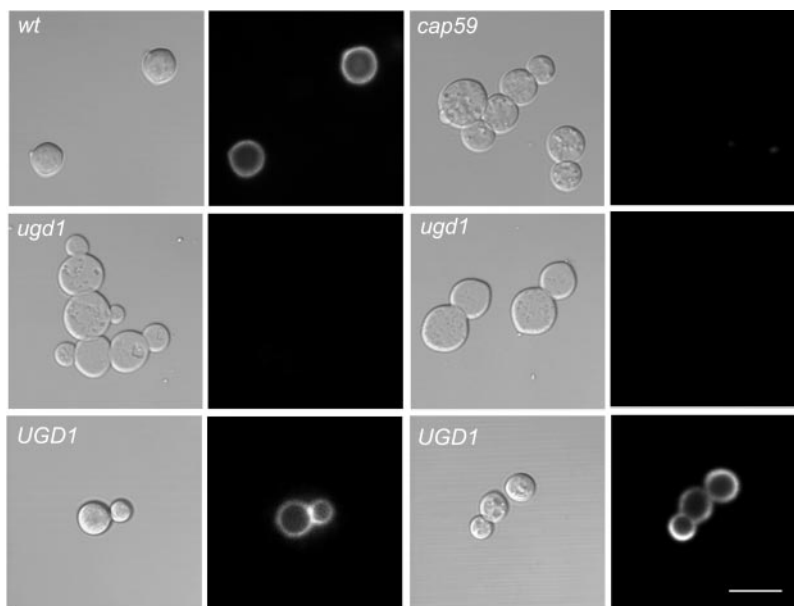
flanking the deletion were maintained (Fig. 1, panel A). After biolistic transformation of this construct into serotype D strain JEC21, we screened drug-resistant transformants by PCR (Fig. 1, panel B). Two of 100 transformants tested had undergone the desired gene replacement. As shown for one of these, the disrupted strain no longer contains the deleted region of *UGD1* but has gained *nat1* sequence. We confirmed the gene disruption by DNA blotting (Fig. 1, panel C, and data not shown). We further subjected one disruptant to biolistic transformation

with a DNA fragment containing the wild type gene adjacent to a second drug resistance marker (see "Experimental Procedures"); this resulted in correction of the deleted gene back to wild type (Fig. 1, panels B and C).

To examine protein expression in the disruption and corrected strains, we used an antibody generated against bacterially expressed *C. neoformans* Ugd1p (8). As shown in Fig. 2, no protein was detected in the disruption strain, although it was present in the corrected version of that strain. This shows that, as expected, disruption of *UGD1* resulted in absence of its protein product.

To confirm that disruption of *UGD1* indeed altered the levels of UDP-GlcUA, we analyzed the nucleotide sugars present in the wild type, *ugd1* disruption, and corrected strains by mass spectrometry. We additionally tested a strain in which the gene encoding UDP-glucuronic acid decarboxylase (*UXS1* (27)) had been deleted (6). These *uxs1* mutant cells should produce UDP-GlcUA but will be unable to convert it to UDP-xylose. As shown in Fig. 3, panel A, and in Table I, both UDP-GlcUA (579.0611) and UDP-Xyl (535.0706) are detected in wild type cells. Cells lacking *Uxs1p*, as expected, produce UDP-GlcUA but no UDP-

FIG. 4. *ugd1* mutant cells are enlarged, deformed, and do not bind anticapsular antibodies. Each image pair shows differential interference contrast (DIC) on the left and confocal immunofluorescence after exposure to Cy3-labeled anticapsular antibody 2H1 at the right. *wt*, wild type cells with normal capsule; *cap59*, an acapsular mutant; *ugd1*, cells disrupted in the gene encoding UDP-glucose dehydrogenase (two fields shown); *UGD1*, correction of *ugd1* described in the text (two fields shown). Scale bar (lower right) corresponds to 10 μ m; all panels are at the same magnification.



xylose (Fig. 3, panel B and Table I). The inability to convert UDP-GlcUA to UDP-xylose in these cells results in accumulation of enormous levels of UDP-GlcUA, dwarfing the other nucleotide sugars (Fig. 3, panel B). Finally, cells in which the *UGD1* gene is disrupted produce no detectable UDP-GlcUA or UDP-xylose (Fig. 3, panel C, and Table I). These results indicate that under the growth conditions employed, in which glucose serves as the major carbon source, Ugd1p serves as the sole provider of UDP-GlcUA to the cell. Cells in which the *ugd1* mutation has been corrected (*UGD1*, Fig. 3, panel D, and Table I) again show the presence of UDP-Xyl and UDP-GlcUA.

The nucleotide sugar analysis presented above demonstrates that *C. neoformans* grown on glucose, as in our standard conditions and in the mammalian host, does not produce UDP-GlcUA by any pathway besides that mediated by Ugd1p. However, an alternative pathway for UDP-GlcUA synthesis has been demonstrated in plants (28, 29), in which an inositol oxygenase (30–33) first converts inositol to GlcUA. This may then be converted to UDP-GlcUA by the sequential actions of a glucuronokinase and a UDP-GlcUA pyrophosphorylase. A non-pathogenic species of *Cryptococcus*, *Cryptococcus lactativorus*, has been shown to contain a functional inositol oxygenase, whose activity is detected when cells are grown on inositol but not when they are grown on glucose (34). As a close homolog of the gene encoding the *C. lactativorus* inositol oxygenase is present in *C. neoformans* genome sequence (34), we measured nucleotide sugar levels in *ugd1* mutant cells grown on minimal medium containing inositol. We were unable to detect any UDP-GlcUA or UDP-Xyl production in these cells, indicating that the alternative pathway for UDP-GlcUA synthesis is not functional in these conditions. Control *ugd1* cells grown on the same medium with glucose as a carbon source also showed no production of these compounds, whereas wild type cells grown on the same medium with inositol as the carbon source demonstrated normal synthesis of nucleotide sugars (not shown).

The disruption of *UGD1*, and resulting reduction of UDP-GlcUA available to the cells, led to several phenotypic alterations. We observed that colonies of the *ugd1* mutant cells appeared dull when grown on solid media, instead of exhibiting the shiny surface typical of this encapsulated fungus. They also grew in clumps in liquid culture, rather than as the dispersed single or budding cells uniformly seen with wild type strains (Fig. 4, compare DIC panels for *ugd1* and *wt*). Both dull colonies and clumping are typical of cells with reduced or absent

capsule (Fig. 4, DIC panel of *cap59*). Finally, microscopic examination showed that the *ugd1* mutant cells were enlarged and had broadened bud necks (compare budding cells in DIC images of *ugd1* to those of the corrected mutant, *UGD1*).

We expected alterations in capsular polysaccharides to result from the *ugd1* mutation and consequent changes in nucleotide sugar availability. We therefore examined cells for the presence of capsule by probing their surfaces with a monoclonal antibody to GXM. As shown in Fig. 4, this antibody (2H1) binds well to the surfaces of wild type cells (*wt*) but does not bind to a known acapsular mutant, *cap59*. We could not detect any binding of 2H1 antibody to the surface of *ugd1* mutants, although the corrected cells (*UGD1*) regained the ability to bind. We next took advantage of a series of monoclonal antibodies to GXM that have been characterized in terms of their broad requirements for binding (35, 36). We tested these antibodies on the *ugd1* mutant, using as controls wild type and acapsular cells as well as several mutants known to lack specific GXM components: *cas2*, which lacks GXM 6-*O*-acetylation (37), and *uxs1*, which lacks xylose residues in GXM (6). The data summarized in Table II show that none of these antibodies clearly bound to the surface of *ugd1* mutant cells, although they exhibited the expected staining pattern for the other strains tested (36).

We expect *ugd1* cells to lack all GXM side chains as well as the xylose residues of GalXM. It is therefore difficult to interpret the observed lack of monoclonal antibody binding to the cell surface. One possibility is that the result indeed indicates an absence of capsule altogether, perhaps because the altered polysaccharide is not made, not stable, or not appropriately localized. Alternatively, the absence of detectable capsule could reflect changes in capsule components such that the antibodies tested, whose specific epitopes are not known, cannot recognize the resulting structure.

To investigate the possible presence of capsule material in a manner independent of antibody reagents, we turned to electron microscopy. Wild type cells (*wt*) examined by this technique are decorated with radiating fibers of capsule material (Fig. 5), in contrast to a known acapsular mutant (*cap59* (38)), which shows a smooth cell wall with no apparent surrounding material. Although the disruption strain (*ugd1*) appeared initially similar to the acapsular one, closer examination revealed a ragged layer of material at the cell surface (compare *ugd1* inset to *cap59* inset). This could represent some aberration of the cell wall or residual capsule material that cannot adopt a

TABLE II
Monoclonal antibody binding to wild type and mutant *Cryptococcus* strains

Results shown are from at least three independent tests of each combination.

Antibody	Requires <i>O</i> -acetylation	Requires xylose	Wild type	<i>cas2</i>	<i>uxs1</i>	<i>ugd1</i>	<i>cap59</i>
1255	No	No	+ ^a	+ ^b	+	– ^c	–
339	Yes	No	+	–	+	–	–
1326	Yes	No	+	–	+	–	–
3C2	No	Yes	+	+	–	–	–
F12D2	No	Yes	+	+	–	–	–

^a Unless otherwise indicated (see notes below), + indicates uniform ring staining of the cell surface with the indicated antibody and – indicates no detectable staining.

^b The bright surface staining seen with antibody 1255 on *cas2* cells had a consistently punctate character, unlike the smoother appearance of this antibody on wild type or *uxs1* cells.

^c *ugd1* cells showed extremely faint staining of their surfaces with antibody 1255 in most experiments, a subtle but consistent difference from the acapsular strain *cap59* (see “Discussion”).

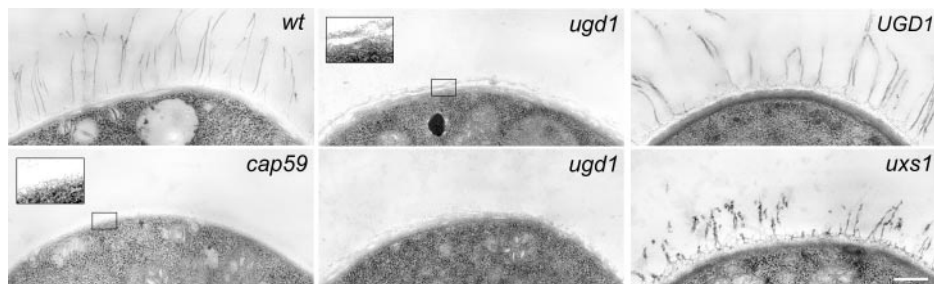


FIG. 5. **Electron microscopy shows altered cell surface appearance in wild type and mutant cryptococci.** Cells were processed as under “Experimental Procedures,” and representative images were chosen to demonstrate phenotype. Strain abbreviations are as in Fig. 4, with the addition of *uxs1*, a mutant in the gene encoding UDP-glucuronic acid decarboxylase. Boxes in two of the panels indicate a portion of the image that was expanded 2.5-fold to demonstrate structure in more detail. Scale bar (lower right) corresponds to 0.25 μm ; all panels are at the same magnification.

normal conformation (see “Discussion”). This phenotype reverts to wild type in the corrected cells (*UGD1*). By contrast, cells defective in UDP-xylose production (*uxs1*) clearly bear capsular material on their surfaces, although the capsule fibers are truncated and thickened.

C. neoformans sheds capsule material into its surroundings, whether the natural environment or an infected host. This material may be recovered and analyzed for composition and structure (25). We therefore used carbohydrate analysis to examine the ability of *ugd1* cells to release capsule components. GXM was readily isolated from wild type cells and the corrected disruption strain, and showed the expected composition and NMR signals (data not shown). By contrast, the same protocol yielded only limited material from *ugd1* disruptant cells (<2% of the mass of polysaccharide obtained from the same number of cells). This material contained mannose, galactose, and glucose in a 4:3:2 ratio,² but NMR analysis (not shown) indicated an absence of any signals typical of the mannose in α -1,3 linkage that constitutes the GXM backbone. The most likely explanation for these results is that the small amount of material obtained from the mutant cells actually originated from cell wall polymers and perhaps truncated GalXM, rather than from the GXM component of capsule. In similar polysaccharide preparations from cells with normal capsule, neutral polymers from cell wall or GXM are not detected, probably due to the great abundance of GXM (for which the isolation procedure is designed).

Cells lacking capsule grow normally in a range of temperatures and growth media. Unlike these acapsular strains, however, the *ugd1* disruption showed somewhat slowed growth at 30 °C and clearly impaired growth at 37 °C (Fig. 6, top panels). The *ugd1* mutant was completely unable to grow when subjected to additional stress, such as growth at pH 8.8 or in the

presence of 1 M NaCl (not shown), growth at 37 °C on minimal medium (not shown), or growth at 37 °C on medium containing low amounts of SDS or Congo Red (Fig. 6). Growth was not changed by lowering the temperature to 25 °C or supplementing the plates with sorbitol as an osmotic support (not shown). Consistent with this temperature sensitivity and poor response to stress, *ugd1* cells were unable to survive in an inhalational model of cryptococcosis in mice (not shown). In all cases the corrected *ugd1* mutant strain grew as wild type (Fig. 6 and data not shown).

Capsule production is not required for normal growth at 37 °C. For this reason the altered growth observed in mutant cells, as well as the observed morphological defects, must be due to some other role of UDP-GlcUA within the cell. *In vitro* radiolabeling experiments of washed membrane preparations suggested that xylose and probably also GlcUA are incorporated from the corresponding nucleotide sugars into proteins and lipids in wild type *C. neoformans* (not shown), but which individual compound gives rise to any observed phenotype is difficult to assess (see “Discussion”).

Finally, we examined the localization of Ugd1p. Although the primary amino acid sequence suggests that this protein should be soluble, consistent with its localization when expressed in *Escherichia coli* (8), there is precedent in other systems for the compartmentalization of proteins involved in nucleotide sugar interconversion (39). Interestingly, the great majority of Ugd1p was membrane-associated (Fig. 7). This suggests that the synthesis of UDP-GlcUA is primarily located at membrane-bounded compartments, perhaps for efficient use in reactions of glycoconjugate synthesis.

DISCUSSION

We initiated the studies detailed above to investigate the effect on cryptococcal biology of reducing levels of the important nucleotide sugar UDP-GlcUA. We initially assumed that this compound was derived from UDP-glucose via UDP-glucose dehydrogenase (Ugd1p), and we therefore disrupted the corre-

² Trace xylose was also detected, but based on the mass spectrometry data and water testing we believe this was a contaminant acquired during sample preparation.

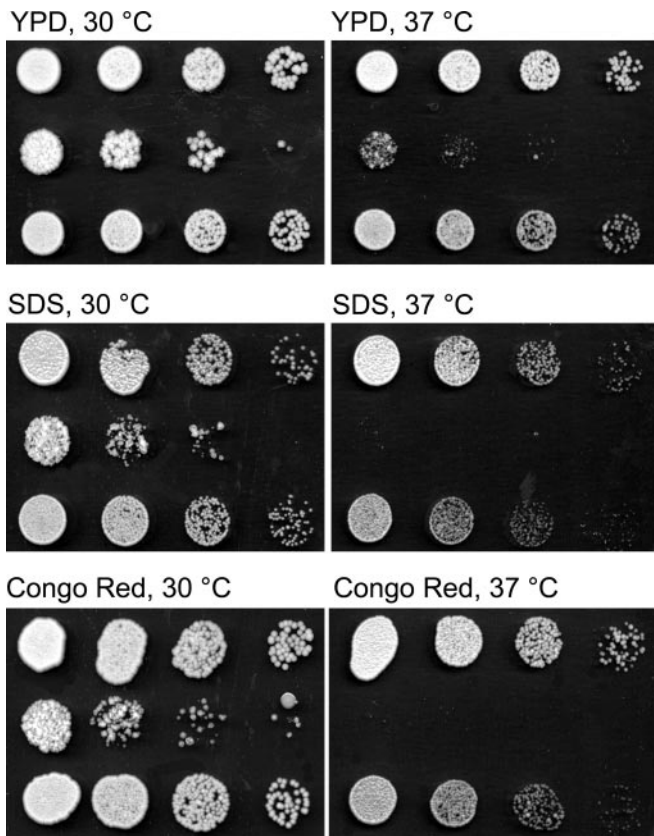


FIG. 6. *ugd1* mutants demonstrate a growth defect under stress. Serial 5-fold dilutions were spotted at the indicated temperatures as described under the "Experimental Procedures," using rich medium (YPD), or the same medium containing 0.005% SDS or 30 μ g/ml Congo Red. In each panel the 1st row is wild type cells, the 2nd row is the *ugd1* disruption, and the 3rd row is the corrected disruption strain. At 37 °C the minimal growth on YPD of the *ugd1* mutant is completely abolished by the other medium additives.

sponding *C. neoformans* gene (*UGD1*). Analysis of the disruptants by immunoblotting indicated lack of the protein, and mass spectrometry showed that UDP-GlcUA had indeed been reduced to below detectable levels.

We further investigated whether stimulation of a potential alternative pathway for UDP-GlcUA synthesis, beginning with inositol oxygenase, might allow some recovery of UDP-GlcUA levels. *ugd1* mutant cells grown on inositol did show minor phenotypic improvements compared with growth on glucose; they grew in culture in a somewhat less clumpy fashion, and colonies recovered a slightly shiny appearance. However, we were unable to detect UDP-GlcUA or UDP-Xyl synthesis in these cells, and we conclude that these alterations are due to other effects of growth on inositol, such as alteration of signal transduction pathways as well as sugar metabolism. In any case, it is clear that UDP-GlcUA is indeed generated by Ugd1p during growth on glucose, which is the situation in most experimental conditions as well as during colonization of mammalian hosts in the setting of cryptococcal disease.

An unexpected observation on Ugd1p that was made in the course of these studies is its apparent membrane localization. There is no signal in the polypeptide sequence typical of membrane association or anchorage, which suggests indirect association with the membrane via interactions with another protein. We have noted similar localization for the cryptococcal Uxs1p,³ which is responsible for UDP-xylose synthesis (27). An

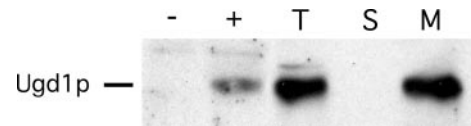


FIG. 7. Ugd1p is primarily found associated with membranes. Wild type cells were fractionated as described under the "Experimental Procedures" and probed with antibody generated against Ugd1p expressed in *E. coli* (8). -, *E. coli* expressing vector alone; +, *E. coli* expressing Ugd1p; T, total protein; S, soluble fraction; M, membrane fraction. Material from equal numbers of cells was loaded in each of the last three lanes.

attractive possibility is that both of these enzymes are present in some type of membrane-associated complex to promote efficient capsule synthesis, but supporting this hypothesis will require further investigation.

Cells lacking Ugd1p, and therefore unable to produce UDP-GlcUA, exhibit multiple defects beyond altered capsule synthesis. They are temperature-sensitive, have impaired cell integrity (as judged by the effect of the cell wall-disrupting agent Congo Red or low levels of SDS), show increased size and morphological defects at the bud neck, and do not survive in mice. We do not know whether these alterations are due to one or more cellular pathways, although because cells that are acapsular due to other mutations do not exhibit these phenotypes, we know they are not due to the capsule impairment. UDP-GlcUA or its downstream products could potentially contribute to important modifications of proteins, lipids, or other glycoconjugates. Our preliminary experiments indicate that GlcUA and Xyl are incorporated into multiple protein and lipid species, but identifying which of these is relevant to the observed phenotypes will be a challenge for the future.

An intriguing question raised by our studies is whether any GXM-related polymer is made in *ugd1* mutant cells. There are at least three possibilities supported by our results that cannot be distinguished in the context of our current understanding of capsule synthesis. One is that in the absence of side chain donors the backbone of GXM is not extended, and the polymer is either not made at all or is not stable. A second model is that the backbone of GXM, either an undecorated or an acetylated mannan, is indeed generated within the cell but is not properly exported to the surface. In these first two cases the altered cell surface seen in electron micrographs would not be due to aberrant capsule material but would instead reflect a defect in cell wall organization, consistent with some of the phenotypic alterations noted in the mutant cells. A third possibility is that some abbreviated form of the molecule does indeed arrive at the cell surface, but does not efficiently react with available antibodies at that site and is either not shed into the medium or is not recovered in the precipitation methods we used. The last model would be consistent with the EM images reflecting the presence of aberrant capsule material at the cell surface. It is notable that extremely faint staining of *ugd1* cell surfaces was seen with one anticapsular antibody. If this antibody is completely unreactive with any cell wall component, this result would support the third model. However, as the specific epitope has not yet been determined, and the staining was extremely faint compared with wild type cells, we cannot yet rule out the other two.

Which of the possible scenarios described above actually occurs depends on the as yet incompletely understood events required to generate GXM. For example, we do not know the site or sites of capsule biosynthetic events or whether capsule components lacking side chains are stable and can be assembled at the cell surface. Distinguishing between various models will require further studies of capsule biosynthesis combined with careful cell fractionation and structural analyses but will

³ C. L. Griffith and T. L. Doering, unpublished results.

ultimately add to our understanding of the fascinating biosynthetic pathway of this critical virulence factor.

Acknowledgments—We thank Guilhem Janbon for encouraging us to use drug markers for gene disruption and for providing strains; Tom Kozel and Arturo Casadevall for monoclonal antibodies; Randy Schekman for polyclonal antibody; June Kwon-Chung and Joe Heitman for strains; and Gary Cox for plasmids. We appreciate the expert assistance of Wandy Beatty and Lori LaRose with the electron microscopy and confocal imaging. We are grateful to Jeramia Ory for suggesting we analyze mutant cells grown on inositol. We thank Jeramia Ory and Aki Yoneda for comments on the manuscript. We also thank Indrani Bose for helpful discussion on analysis of gene disruptions and all the members of the Doering lab for useful discussions and suggestions.

REFERENCES

- Seifert, G. J. (2004) *Curr. Opin. Plant Biol.* **7**, 277–284
- Nummila, K., Kilpelainen, I., Zahringer, U., Vaara, M., and Helander, I. M. (1995) *Mol. Microbiol.* **16**, 271–278
- Zabackis, E., Huang, J., Muller, B., Darvill, A. G., and Albersheim, P. (1995) *Plant Physiol.* **107**, 1129–1138
- Vaishnav, V. V., Bacon, B. E., O'Neill, M. O., and Cherniak, R. (1998) *Carbohydr. Res.* **306**, 315–330
- Cherniak, R., Valafar, H., Morris, L. C., and Valafar, F. (1998) *Clin. Diagn. Lab. Immunol.* **5**, 146–159
- Moyrand, F., Klaproth, B., Himmelreich, U., Dromer, F., and Janbon, G. (2002) *Mol. Microbiol.* **45**, 837–849
- Campbell, R. E., Mosimann, S. C., van De Rijn, I., Tanner, M. E., and Strynadka, N. C. (2000) *Biochemistry* **39**, 7012–7023
- Bar-Peled, M., Griffith, C. L., Ory, J. J., and Doering, T. L. (2004) *Biochem. J.* **381**, 131–136
- Schiller, J. G., Lamy, F., Frazier, R., and Feingold, D. S. (1976) *Biochim. Biophys. Acta* **453**, 418–425
- Gainey, P. A., Pestell, T. C., and Phelps, C. F. (1972) *Biochem. J.* **129**, 821–830
- Franzen, J. S., Ashcom, J., Marchetti, P., Cardamone, J. J., and Feingold, D. S. (1980) *Biochim. Biophys. Acta* **614**, 242–255
- Jaenicke, R., and Rudolph, R. (1986) *Biochemistry* **25**, 7283–7287
- Franzen, J. S., Marchetti, P. S., Lockhart, A. H., and Feingold, D. S. (1983) *Biochim. Biophys. Acta* **746**, 146–153
- Davidson, R. C., Blankenship, J. R., Kraus, P. R., De Jesus Berrios, M., Hull, C. M., D'Souza, C. A., Wang, P., and Heitman, J. (2002) *Microbiology* **148**, 2607–2615
- McDade, H. C., and Cox, G. M. (2001) *Med. Mycol.* **39**, 151–154
- Toffaletti, D. L., Rude, T. H., Johnston, S. A., Durack, D. T., and Perfect, J. R. (1993) *J. Bacteriol.* **175**, 1405–1411
- Davidson, R. C., Cruz, M. C., Sia, R. A. L., Allen, B., Alspaugh, J. A., and Heitman, J. (2000) *Fungal Genet. Biol.* **29**, 38–40
- Cox, G. M., Toffaletti, D. L., and Perfect, J. R. (1996) *J. Med. Vet. Mycol.* **34**, 385–391
- Ausubel, F. M., Brent, R., Kingston, R. E., Moore, D. D., Seidman, J. G., Smith, J. A., Struhl, K., Albright, L. M., Coen, D. M., and Varki, A. (2004) in *Current Protocols in Molecular Biology* (Chanda, V. B., ed) Vol. 1, pp. 2.9.1–2.9.11, John Wiley & Sons, Inc., New York
- Rabina, J., Maki, M., Savilahti, E. M., Jarvinen, N., Penttila, L., and Renkonen, R. (2001) *Glycoconj. J.* **18**, 799–805
- Hwang, H. Y., and Horvitz, H. R. (2002) *Proc. Natl. Acad. Sci. U. S. A.* **99**, 14218–14223
- Zhang, L., Beeler, D. L., Lawrence, R., Lech, M., Liu, J., Davis, J. C., Shriver, Z., Sasisekharan, R., and Rosenberg, R. D. (2001) *J. Biol. Chem.* **276**, 42311–42321
- Pierini, L. M., and Doering, T. L. (2001) *Mol. Microbiol.* **41**, 105–115
- Merkle, R. K., and Poppe, I. (1994) *Methods Enzymol.* **230**, 1–15
- Cherniak, R., Morris, L. C., Anderson, B. C., and Meyer, S. A. (1991) *Infect. Immun.* **59**, 59–64
- Sommer, U., Liu, H., and Doering, T. L. (2003) *J. Biol. Chem.* **278**, 47724–47730
- Bar-Peled, M., Griffith, C. L., and Doering, T. L. (2001) *Proc. Natl. Acad. Sci. U. S. A.* **98**, 12003–12008
- Sasaki, T., and Taylor, I. E. P. (1984) *Plant Cell Physiol.* **25**, 989–997
- Seitz, B., Klos, C., Wurm, M., and Tenhaken, R. (2000) *Plant J.* **21**, 537–546
- Loewus, F., Murthy, P., and Neufeld, E. (1962) *Proc. Natl. Acad. Sci. U. S. A.* **48**, 421–425
- Reddy, C. C., Pierzchala, P. A., and Hamilton, G. A. (1981) *J. Biol. Chem.* **256**, 8519–8524
- Reddy, C. C., Swan, J. S., and Hamilton, G. A. (1981) *J. Biol. Chem.* **256**, 8510–8518
- Arner, R. J., Prabhu, K. S., Thompson, J. T., Hildenbrandt, G. R., Liken, A. D., and Reddy, C. C. (2001) *Biochem. J.* **360**, 313–320
- Kanter, U., Becker, M., Friauf, E., and Tenhaken, R. (2003) *Yeast* **20**, 1317–1329
- Belay, T., Cherniak, R., Kozel, T. R., and Casadevall, A. (1997) *Infect. Immun.* **65**, 718–728
- Kozel, T. R., Levitz, S. M., Dromer, F., Gates, M. A., Thorkildson, P., and Janbon, G. (2003) *Infect. Immun.* **71**, 2868–2875
- Janbon, G., Himmelreich, U., Moyrand, F., Improvisi, L., and Dromer, F. (2001) *Mol. Microbiol.* **42**, 453–467
- Chang, Y. C., and Kwon-Chung, K. J. (1994) *Mol. Cell. Biol.* **14**, 4912–4919
- Harper, A. D., and Bar-Peled, M. (2002) *Plant Physiol.* **130**, 2188–2198